

From Waves to Touch: Advancing Ultrasound Haptics through Novel Modulation

Mohammed H. Rasheed

Thesis submitted to the Faculty of the
Virginia Polytechnic Institute and State University
in partial fulfillment of the requirements for the degree of

Master of Science
in
Mechanical Engineering

Shima Shahab, Chair

Raffaella De Vita

Wynn Legon

Adam D. Maxwell

September 24, 2025

Blacksburg, Virginia

Keywords: Ultrasound haptics, Ultrasound, Touch sensation, Elastic waves, Modulation
techniques

Copyright 2025, Mohammed H. Rasheed

From Waves to Touch: Advancing Ultrasound Haptics through Novel Modulation

Mohammed H. Rasheed

(ABSTRACT)

Ultrasound-based mid-air contactless haptics have been an increasingly popular area of development in the past decade for their highly valuable applications in VR environments, automobile safety systems, surgical training environments, and public displays. While currently applied modulation techniques such as amplitude- and spatiotemporal-modulation (AM and STM) can elicit sensations in the human skin for 2D shapes, there is still much to be desired in terms of spatial precision for high-speed scanning points. Specifically, when points are scanned across the human palm at speeds greater than the shear speed of sound, a trailing Mach cone is produced behind the focal point, leading to poor localization and inaccurate shape perception. In this work, time-domain acoustic simulations of an approximate elastic skin model are used to i) characterize a pre-existing modulation technique termed AM-STM and display its increased localization capabilities in comparison to the other pre-existing methods, and ii) introduce and define a new modulation technique termed SM-STM which has displayed further increased localization and improved perception.

From Waves to Touch: Advancing Ultrasound Haptics through Novel Modulation

Mohammed H. Rasheed

(GENERAL AUDIENCE ABSTRACT)

Haptic devices are instruments which give interactive feedback to a user based on certain commands, primarily through the sense of touch. Humans in the modern day interact with haptic devices on a regular basis, whether that be the simple vibration experienced from a cellphone notification or gaming controller, or an interactive display at a museum. However, haptics have many other applications which are not as common, such as touch-based feedback for prosthetics, surgical training for doctors, automobile feedback safety systems, and devices for the sensorially impaired. Recently, ultrasound-based mid-air haptic systems have been developed with the purpose of creating a more immersive experience. These systems have shown to elicit the sense of touch in humans by generating acoustic pressure fields in mid-air which can be felt by a user. This allows the user to seemingly feel an object, while no object is “truly there.” However, the acoustic pressure points alone cannot be felt by the neural mechanisms in our skin, and thus, various modulation techniques must be applied in order for a sensation to be felt. In this work, a time-domain model is used to characterize and further understand a previously established modulation technique, and define a new modulation technique that can further improve sensation.

Dedication

This work is dedicated to my parents, Prof. Hayder Rasheed and Dr. Fatma Radhi, MD. who were great examples in my life which shaped me into the man I am today. Thank you for your sacrifices, encouragement, and constant support.

Acknowledgments

I would first and foremost like to thank God for all of the blessings and opportunities that I have been given in my life, and for blessing me with the position that I am in to be able to submit this thesis. I furthermore would like to express my utmost gratitude and thanks to my research advisor, Prof. Shima Shahab, whose wisdom, patience, and encouragement has left me with nothing short of a positive effect in my life. Her unwavering support and belief in me throughout the research process is truly appreciated. Dr. Shahab's commitment to helping her students at every moment in the research process is unlike any other, and is a big contributor to the success of this research. Dr. Shahab continued to believe in me during both the easy and difficult times, and for that I am beyond grateful. I also extend my thanks to my thesis committee members, Profs. Raffaella De Vita, Adam Maxwell, and Wynn Legon, whose intellect and excitement for this thesis topic helped motivate me throughout the research process. I lastly would like to share my thanks to my invaluable lab mates at MInDS lab, both past and present. Dr's Ahmed Sallam, Ravi Bollineni, Moustafa Sayed Ahmed, and Jiaxin Xi, as well as (soon to be Dr's) Hrishikesh Kulkarni, Ceren Cengiz, and Mihir Pewekar. I truly could not have asked for a better environment to conduct this research in. Being constantly surrounded by highly smart, hard-working, and kind people surely helped me along this research journey. This dissertation was partially supported by the U.S. National Science Foundation (NSF) under Grant No. CAREER CMMI 2143788, which is gratefully acknowledged.

Contents

List of Figures	vii
1 Introduction to Objectives and Background	1
1.1 Purpose	1
1.2 Objectives	1
1.3 Review of Literature	2
1.3.1 Focused Ultrasound	2
1.3.2 Origins of Haptics	5
1.3.3 Fundamentals of Mechanoreceptors	10
2 Dynamic Modulation of Shear Shock Waves in Tissue to Advance Spatial Precision in Ultrasound Haptics	14
2.1 Introduction	14
2.2 System Model	18
2.3 Results and Discussion	19
2.4 Conclusion	30
Bibliography	31
3 Future Work	43

List of Figures

1.1	Transcranial focused ultrasound (FUS) administered using a curved transducer. [28]	3
1.2	Visualization of the primary three focal point modulation techniques. [36]	9
1.3	Visualization of mechanoreceptor locations in the human skin. [10]	12
1.4	Right: FEM model [32]. Mechanoreceptor models available in the literature. Left: TouchSim continuum mechanics model [60]. Bottom: Resistor network model [53].	13
2.1	A schematic representation of the system, including a backing material, illustrating the focal point characterized by a Gaussian distribution with a variable full width at half maximum (FWHM).	18
2.2	k-Wave simulation results of the out-of-plane displacement of the tissue-like material for different focal point scanning speeds. The ultrasound focal point is modeled as a displacement boundary with a spatial Gaussian distribution, with FWHM values of 2 mm (upper row) and 6 mm (lower row). In the case of scanning of a 2 mm FWHM focal point at 7 m/s, the out-of-plane displacement is recorded to be in the range of 2.19 μm and -3.34 μm . A normalized color bar is used for comparison purposes across all scanning scenarios. The figure also includes the FFT results of the displacement at the center of the tissue-like material.	19

2.3	<p>(a) A schematic of the system showing a moving focal point along a straight line, with the signal applied to the focal point being amplitude-modulated.</p> <p>(b) Normalized out-of-plane displacement of the tissue-like material surface at a fixed time, with the Gaussian point source swept along a linear path at a speed of 7 m/s; each plot corresponds to a different modulation frequency, with an ultrasound excitation carrier frequency of 40 kHz.</p> <p>(c) Reconstruction efficiency (η) as a function of simulation time, with the point source sweeping from left to right across the tissue-like material surface at different modulation frequencies.</p> <p>(d) Inverse participation ratio (IPR) as a function of simulation time.</p> <p>(e) The η and IPR values extracted at 14 ms (steady state) from (c) and (d) as a function of modulation frequency.</p>	20
2.4	<p>(a) A schematic of the system showing a moving focal point along a straight line, with the signal applied to the focal point, and the spatial position of the point as a function of time.</p> <p>(b) η and IPR as a function of simulation time, with the point source sweeping from left to right across the tissue-like material surface at different frequencies of speed oscillation.</p> <p>(d) The η and IPR values extracted at 14 ms (steady state) from (b) as a function of the frequency of speed oscillation.</p>	21
2.5	<p>(a) FFT analysis of the out-of-plane displacement at the center of the tissue-like material using the AM-STM technique with a scanning speed of 7 m/s at different modulation frequencies.</p> <p>(b) Similar analysis for the SM-STM technique with a variable sinusoidal scanning speed, averaging 7 m/s, at different speed frequencies</p>	21

2.6	(a1,a2) A schematic of a 40 kHz input signal applied as a pin indentation to the center of the palm, marked by a large gray circle, which has a 2mm diameter (not shown to scale). (a3) Spatial representation of fired PC afferents, displaying the location of where receptors were activated throughout the hand. (a4) Spike raster plot which shows the neurons which are fired in the palm with respect to time. A zoomed-in image of the graph displays greater detail of the temporal spread of activated receptors, since all of the receptors are fired within the first 0.015 seconds. (b1,b2) Similar to 2.6a, a schematic is shown of a 200 Hz AM input signal applied as a pin indentation to the center of the palm, marked by a large gray circle, which has a 2mm diameter (not shown to scale). (b3) Spatial representation of fired PC afferents, displaying the location of where receptors were activated throughout the hand. (b4) Spike raster plot which shows the neurons which are fired in the palm with respect to time. In this scenario, it is shown that neurons are fired throughout the entire duration of the input signal.	27
2.7	(a) The desired input signal for STM which is obtained from k-Wave simulations. (b) General location of the scanned input signal along the palm. Gray circles which are numbered 1-5 represent locations where neural response data was recorded/observed. (c) Spatial representation of fired neurons on the surface of the palm. (d) Plots relating to the input displacement (top) and neural response (bottom) at the 5 mentioned locations in 2.7b. A clear time delay in neuron firing can be seen in plots 2-4, which is expected for the moving points which reaches the consecutive locations after a certain time.	28
3.1	Experimental set up, missing reflective powder on the surface of the gel . . .	44

List of Abbreviations

AHL Acoustic Holographic Lens

AM Amplitude Modulation

AM-STM Amplitude-Modulated Spatiotemporal Modulation

ARF Acoustic Radiation Force

AUTD Airborne Ultrasound Tactile Display

DTP Dynamic Tactile Pointer

FA1 Fast Adapting Type 1

FA2 Fast Adapting Type 2

FUS Focused Ultrasound

FWHM Full Width at Half Maximum

HCI Human Computer Interaction

IASA Iterative Angular Spectrum Approach

IPR Inverse Participation Ratio

LM Lateral Modulation

PAT Phased Array Transducer

PC Pacinian Corpuscle

SA1 Slow Adapting Type 1

SA2 Slow Adapting Type 2

SM-STM Speed-Modulated Spatiotemporal Modulation

STM Spatiotemporal Modulation

STP Spatio-temporally Modulated Tactile Pointer

VR Virtual Reality

Chapter 1

Introduction to Objectives and Background

1.1 Purpose

The purpose of this thesis is to contribute to the understanding of established modulation techniques used in ultrasound haptics by investigating the resultant viscoelastic wave effects on the human skin and relating them to the perceived sensation. Furthermore, this thesis will explore a new modulation technique and will characterize its expected mechanical response, showing its potential for future use in non-contact ultrasound haptics devices.

1.2 Objectives

As mentioned in section [1.1](#), the general purpose of this thesis is to further explore both established and new modulation techniques in ultrasound haptics. However, this thesis can be further defined by three primary objectives. The main objectives which are presented in this thesis are as follows:

- Model and characterize the previously defined amplitude-modulated spatiotemporal modulation technique.

- Define and model the newly developed speed-modulated spatiotemporal modulation technique.
- Relate the predicted mechanical response(s) to the expected sensation of a potential user.

1.3 Review of Literature

1.3.1 Focused Ultrasound

Ever since the discovery of the piezoelectric effect in the 1880's [34], the field of ultrasound has gained significant attention and progress by researchers in various fields. While unmodified ultrasound waves may be used for a wide variety of applications such as in sensing, imaging, and non-destructive testing/evaluation, it wasn't until the idea/discovery of focused ultrasound (FUS) that caused significant medical treatments and research techniques to emerge. In the modern day, many medical illnesses may be treated with therapeutic FUS. Chaussy et al. were the first to develop shock wave lithotripsy for the treatment of kidney stones as early as the 1980's. Histotripsy was then later developed for precise removal of tissue via non-thermal, purely mechanical means. This was done by using FUS to produce microbubbles in the desired treatment area to destroy unwanted tissue such as tumors [74]. Furthermore, transcranial FUS is an active area of research with the potential to treat conditions such as essential tremor, alzheimer's disease, and brain tumors, among others [24]. Other biomedical research techniques have also emerged with the utilization of FUS such as acoustophoresis for particle/cell separation [46], acoustic tweezers for precise particle/cell manipulation [70], and precise tissue assembly [48]. Furthermore, many non-medical applications have been realized/improved through the means of FUS, with one primary example

being contactless ultrasonic power transfer systems [11] [9] [8].

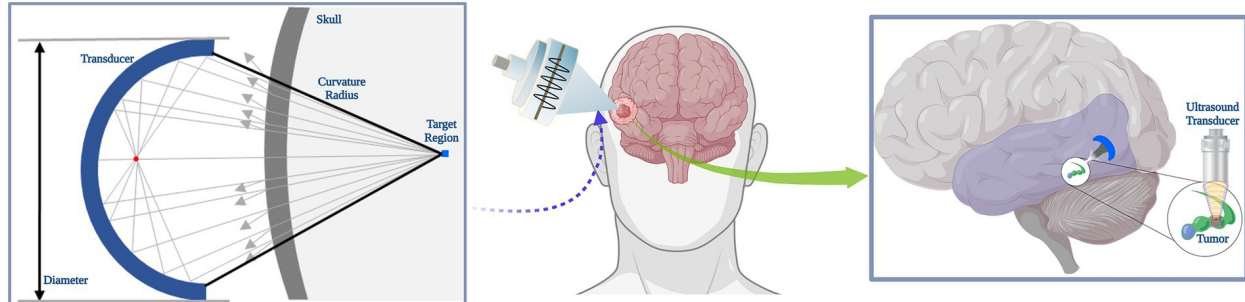


Figure 1.1: Transcranial focused ultrasound (FUS) administered using a curved transducer. [28]

Currently, there are 3 primary methods used for ultrasound focusing. The first method to be discovered was in 1935 [19] which consisted of using a concave surface piezoelectric transducer to create a precise spherical ultrasound focal region. This technique is later used in many medical applications, such as in Transcranial FUS (Fig. 1.1) Furthermore, Phased Array Transducers (PAT's) may be used for a variety of focusing applications. PAT's are capable of generating precise ultrasound focal regions by applying an array of discrete ultrasound transducers which emit ultrasonic waves in a precisely delayed manner. These precise emission delays, or phase shifts, allow for constructive interference to occur in order to generate precise focal regions [67]. PAT's are by far the most utilized for their versatility and active tuning capabilities, with the possibility of real-time control, however some significant limitations include limited spatial resolution and high cost of device production. Acoustic Holographic Lenses (AHL's), on the other hand, offer a suitable solution to these limitations by providing higher spatial resolution and lower cost of production. AHL's are described as engineered metasurfaces that are applied to an ultrasound transducer which can manipulate the outgoing wavefront to any desired shape/pattern. This method was popularized by Melde et al. and can often be computed for various applications in homogeneous media using the Iterative Angular Spectrum Approach (IASA) [47] [63] [61] [3] [4]. AHL's may also

be generated through other techniques using time- and mixed-domain methods [64] [18] for applications in heterogeneous media [62] [17]. Some limitations to AHL's, however, include the inability of active pattern tuning/manipulation.

Acoustic Radiation Force

The acoustic radiation force is a force which appears when an acoustic wave changes its medium. This occurs due to the momentum transfer of the wave between media along the wave path. In the case of acoustic waves traveling from fluid to solid media, such as in the air-skin interface present in haptics, it can be observed that total reflection of the wave will occur. This can further be confirmed by calculation of the reflection coefficient based on acoustic impedance (Eq. 1.1). In the case of the air-skin interface, Z_2 represents the skin impedance and is approximated to be $1.99 \times 10^6 \left(\frac{kg}{sec \cdot m^2}\right)$, and Z_1 is the air impedance which is approximated to be $415 \left(\frac{kg}{sec \cdot m^2}\right)$ [6] [43].

$$r = \frac{(Z_2 - Z_1)}{(Z_2 + Z_1)} \quad (1.1)$$

$$r \approx 0.999$$

Thus, the resultant value for the reflection coefficient (≈ 1) indicates that total reflection will occur. In cases where a wave is perfectly reflected, the radiation pressure applies a force, known as the acoustic radiation force (ARF), on the surface of the reflector (solid), causing it to experience movement or deflections [7][73]. The ARF is generally described mathematically for total reflections as (Eq. 1.2). Here, I is the acoustic intensity at the given location, A is the cross-sectional area of the beam, and c is the longitudinal wave velocity. I is further described with Eq. 1.3, where p refers to the acoustic pressure at the given location, and ρ represents the density of the fluid medium.

$$F = \frac{2AI}{c} \quad (1.2)$$

$$I = \frac{p^2(t)}{2\rho c} \quad (1.3)$$

Here, the relationship between intensity (I) and pressure (p) is nonlinear, thus causing the resulting force to also have the same nonlinear relationship.

1.3.2 Origins of Haptics

Haptic technology is an increasingly popular area of development in the world of progressively complex technological interactions. Haptic feedback refers to various technologies which stimulate/generate the human sense of touch through the use of motions or vibrations on the user's skin, to provide feedback. Something as simple as the vibration of the common smartphone or gaming controller can provide the desired feedback to enhance the common user experience.

Initial concepts of haptics began to emerge as early as the 17th century, as described by Ziat [76]. It is explained that ancient philosophers would use words such as "tactile" and "tactual" to distinguish between physical objects that were subjected to touch and objects of ideas and thoughts (non-physical).

Haptics has since evolved into a field of study pursued by Mechanical and Electrical Engineers, Computer Scientists, Neuroscientists, Psychologists and any area which is interested in further understanding the human sense of touch. Researchers in the field of human-computer interaction (HCI) and Biomedicine have made significant progressions in the understanding and development of haptics and haptic technologies. Primarily, devices in which haptics are

generated via direct contact have received significant attention. Gomez et al. were among the first to develop force-feedback haptic gloves for virtual reality (VR) environments [33]. Similarly, many other wearable haptics such as vests, suits, and chairs have also been produced which rely on vibrational feedback [16, 44, 50]. Wang et al. were further able to successfully design a liquid-vapor based haptic device that is portable and has Braille-producing capabilities [71].

These contact-based haptic technologies have many applications in areas such as VR, automotive, rehabilitation, prosthetics, devices for the sensorially impaired, surgery, and more [1, 13, 14, 25, 42, 55, 69].

In recent years, however, the haptics community has further expanded its development of technology to produce various devices which can generate sensations in the human skin via mid-air means, leading to a more interesting and immersive experience. The primary difference from its former counterpart is that mid-air haptics do not require physical contact, and in some cases, can seemingly construct virtual objects. That is, the user may simply experience touch-based feedback without making physical contact with any device/interface, or even further experiencing the touch of an object in space while there is no solid object present.

Mid-air haptic feedback may be generated through various means. Suzuki et al. were among the first to utilize air jets to send contactless touch signals to users of a virtual reality (VR) system [68]. This was done by utilizing a receiver which is held by the user. Based on the positions of the receiver, air is released from jets placed in the VR environment, which impacts the receiver. The user then experiences pressure as a force from the receiver, and not from the blowing air itself. Shultz et al. and later Shen et al. continued to utilize synthetic jets to facilitate mid-air haptics by more precisely controlling the air output diameter, wind speed, and target pressure, allowing for sensations to occur from just the air alone without

the need for a receiver [66] [65].

Weiss et al developed a mid-air haptic feedback technique known as FingerFlux [72], which utilized electromagnetic fields to elicit sensation on the fingertip. In their work, FingerFlux allowed for near surface mid-air haptics which provided feedback to the user via attractive and repellent forces of electromagnets attached to an “interactive table”. The polarity and strength of the fixed electromagnets may be controlled by a specific software, which would produce attractive and repellent forces to a permanent magnet that is attached to the user’s finger. Furthermore, a light based optical-haptic system was designed by Rekimoto, in which the user would receive haptic feedback in mid-air via a photodetector and piezoelectric actuator attached to the user’s fingertip, called “SenseableRays” [58].

While many of the mentioned techniques are capable of producing sensation in the human skin, the most prominent method for precise sensation generation through mid-air means is by using focused Ultrasound (FUS). Initial discoveries of the ability to use FUS to produce sensation can be found as early as the 1970’s in water/liquid media [29][30][22]. However, it wasn’t until the published work by Iwamoto and Hoshi et al. that began the transition into the modern-day concept known ultrasound haptics [40][41][38][39]. They were among the first to develop original prototypes consisting of phased-array transducers (PAT’s), which they termed the “Airborne Ultrasound Tactile Display” (AUTD) [40][37]. The AUTD utilized a non-linear ultrasound phenomenon known as the “acoustic radiation pressure” to generate tactile sensations via stress fields in 3D free space. Later, more refined, prototypes were developed by Carter et al., known as UltraHaptics [15]. With the initial application of public contactless and interactive tactile displays in mind, the first of these devices was made with increased precision and was compatible with light-based projector displays for enhanced immersive user experience. Since then, UltraHaptics, now known as UltraLeap, has evolved into a well-known startup company in the field of mid-air haptics, with a plethora

of ultrasound-based haptic devices/models.

Both of the mentioned devices/prototypes utilize various modulation techniques applied to ultrasound focal points to generate useful sensations via the acoustic radiation pressure. Generally, a static, unaltered (unmodulated) ultrasound (>20 kHz) focal point can only be perceived during its initial impact on the human skin and cannot be felt long-term. This is mainly due to the initial impact generating low frequency acoustic radiation pressure components, which quickly dissipate, leaving higher ultrasound-range frequencies to remain, which lie outside of the range of sensible frequencies of mechanoreceptors present in the human skin. In order to experience practical, long-term sensation, the focal point must be properly modulated, and is done so by applying 3 primary methods. These three long-standing modulation techniques have been well defined in [36]. Amplitude modulation (AM) is a technique which modulates the static ultrasound foci into a temporally (sinusoidally) varying signal with a lower frequency envelope by changing its amplitude. This lower frequency lies in the perceivable range of mechanoreceptors and can thus be sensed. This technique can be applied to either a single focus or multiple foci distributed in the arrangement of any desired shape. However, this comes at the cost of a weaker sensation due to the total power of the PAT being distributed amongst the multiple foci. Lateral- and Spatiotemporal-modulation (LM and STM) instead generate sensations by moving/scanning a constant amplitude focal point across the surface of the skin. These techniques instead generate sensations due to a temporal change in acoustic radiation pressure on individual stationary mechanoreceptors. That is, while the focal point is moving, any given location on the skin in the trajectory of the scanning path will experience a rapid change in its indentation/deformation in an impulse-like manner. This will then result in the previously mentioned low frequency acoustic radiation pressure components to generate and thus be sensed. LM and STM techniques are often further enhanced by repetitive scanning of focal points along the same trajectory,

which is generally called the “draw frequency”. The draw frequency can be in the range of 25-125 Hz or more and further contributes to sensation by producing an AM-like effect by temporally deforming a given location on the skin at a constant rate in the perceptible frequency range. While both LM and STM techniques work on the same principle, the main difference is that LM, as the name implies, is often restricted to linear motions while STM can consist of any shape. These techniques can be further visualized in Fig. 1.2.



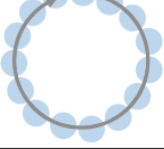
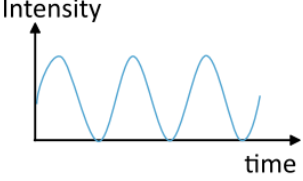
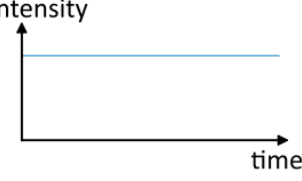
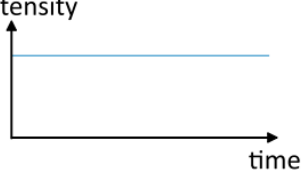
	AM	LM	STM
Focal Trajectory	Immobilized 	Relatively Short Line (up to 2λ for linear LM) 	Variously Scaled 2D Pattern (can be 3λ to 10λ) 
Radiation Force			

Figure 1.2: Visualization of the primary three focal point modulation techniques. [36]

The primary advantage of LM/STM over AM is that instead of distributing the PAT power among many spatially arranged points, the full PAT power can instead be used on one focal point, resulting in a more recognizable sensation. However, a significant weakness of LM/STM is that at high scanning speeds, specifically above that of the shear speed of sound of the skin, a reduced accuracy in perception is found [26]. This is primarily due to the formation of shock waves and is further explained in [56].

Further combinations of the primary modulation techniques have also been proposed. Hajas et al. introduced a combination of AM and STM techniques by applying a slowly moving AM

focal point along the trajectory of a 2D shape [35]. This technique is termed the Dynamic Tactile Pointer (DTP) and is described to produce the feeling of an object being drawn in a continuous brush-like stroke, especially when the focal point speed is slowed at the edges of the shape. Results from their user-study experiments show high shape recognition accuracy for participants in a stationary-hand environment of up to 83%. A further derivative of the DTP is the Spatio-temporally-modulated Tactile Pointer (STP), as introduced by Mulot et al. [49]. Similar to the DTP, the STP would reduce the desired 2D shape into sections of STM segments, allowing for the mentioned benefits of STM to be applied to the technique proposed by Hajas et al., with results showing even further shape perception accuracy.

1.3.3 Fundamentals of Mechanoreceptors

The skin is the largest organ in the human body, and is the interface which translates the sense of touch. In order to improve the sense of touch administered from haptic devices, a solid background knowledge of the internal mechanisms which generate and interpret the sense of touch must be established. The somatosensory system is very complex and contains a variety of sensing mechanisms for both internal and external excitations. The primary receptors which are relevant to this thesis are known as mechanoreceptors, which lie within the dermal layer of the skin, and are responsible for relating information pertaining to external physical indentations and pressures to the brain. These mechanoreceptors fall into four categories and work together to relay information to the brain. These mechanoreceptor types are Slow Adapting types 1 and 2 (SA1 and SA2), known as Merkel cells and Ruffini endings, and Fast/Rapid Adapting types 1 and 2 (FA1 and FA2), known as Meissner and Pacinian corpuscles [23].

Merkel cells (SA1) are often described as the primary group which are responsible for differ-

entiating coarse textures and patterns and are often activated when sustained or when low frequency pressures are applied (>5 Hz) [45][12]. Ruffini endings (SA2) are similar to their other slow-adapting counterpart in that they are activated upon sustained indentations, but cannot pick up on dynamic inputs and are responsible for relaying information related to grip strength. The Meissner corpuscle group (FA1) can sense higher frequencies (5 – 300 Hz) and is described to be able to determine temporal and spatial changes in skin deformation [45]. Pacinian corpuscles (FA2) can sense even higher frequencies (5 – 800 Hz) and is also responsible for understanding temporal changes in the human skin and can furthermore differentiate fine textures [45][23][12].

It is also important to mention the physical depth of mechanoreceptor groups within the human skin. Figure 1.3 gives an accurate depiction of the mechanoreceptors located within the skin, showing the approximate locations of the mentioned mechanoreceptor groups in both hairy and glabrous skin. Glabrous skin is defined as the skin which is hairless and exists in a few locations such as the hand palm and soles of feet. Glabrous skin is often more sensitive, since it contains a higher mechanoreceptor density due to the lack of hair roots present in the surrounding area. As it is shown in the figure, the mechanoreceptor groups are distributed all throughout the dermal layer of the skin, with the PC group having the most depth within the dermal layer, which can be up to 4mm [23].

Within the realm of this work, the primary mechanoreceptor groups which are considered are the Meissner and Pacinian corpuscle (PC) groups. This is mainly because ultrasound administered to the surface of the skin results in higher frequencies which dissipate on its surface, in a range that is picked up by the mentioned groups [15].

Many attempts have been made to accurately model the behavior of mechanoreceptors in response to physical inputs [23]. Gerling et al. produced a 276,000 finite element model of the fingertip, which recorded strain energy density as an input for a leaky integrate-and-fire

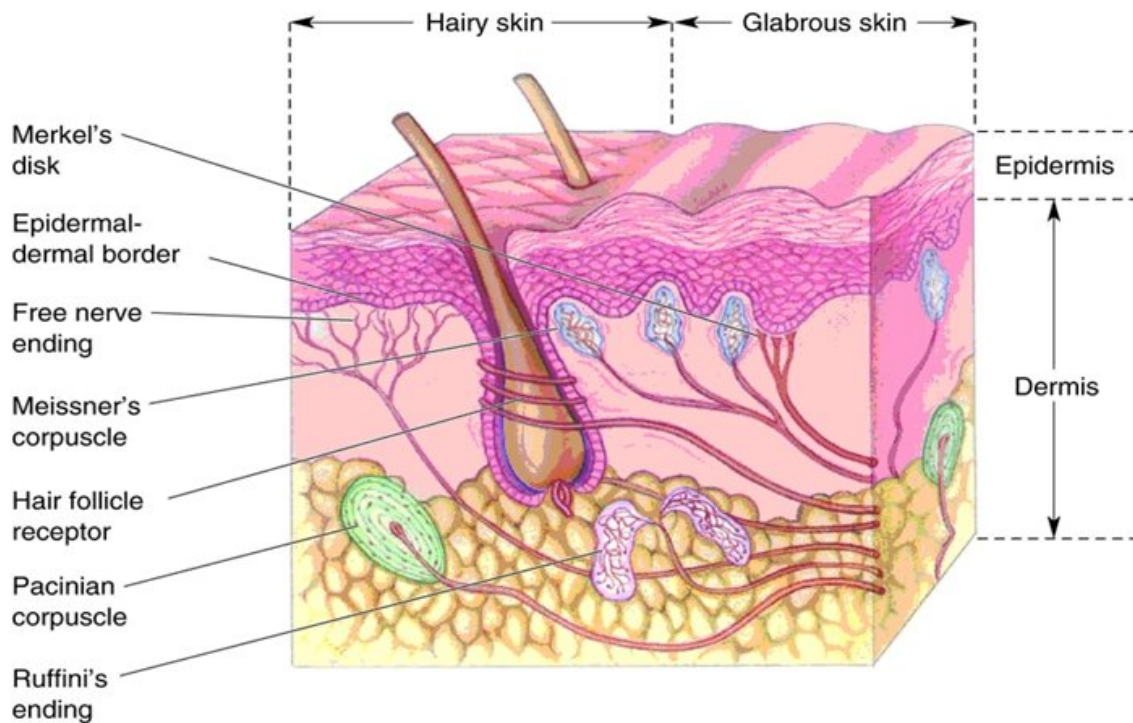


Figure 1.3: Visualization of mechanoreceptor locations in the human skin. [10]

(IF) model for SA1 afferents [32]. While this model provided a detailed representation of the skin mechanical response, it is quite computationally demanding. Saal et al. on the other hand, developed a model which is similar in concept but rather analytically solves for the mechanical inputs using continuum mechanics, which is then also fed into an IF model for neural response [60]. This model allowed for SA1, RA1, and RA2 afferents to be effectively modeled across the whole hand. Ouyang et al. further reduced computation time by assuming that the skin is made up of a resistance network, and related the node voltages at the connection points to the neural response using an IF model [53], which successfully predicted the response of SA1, RA1, and RA2 afferents.

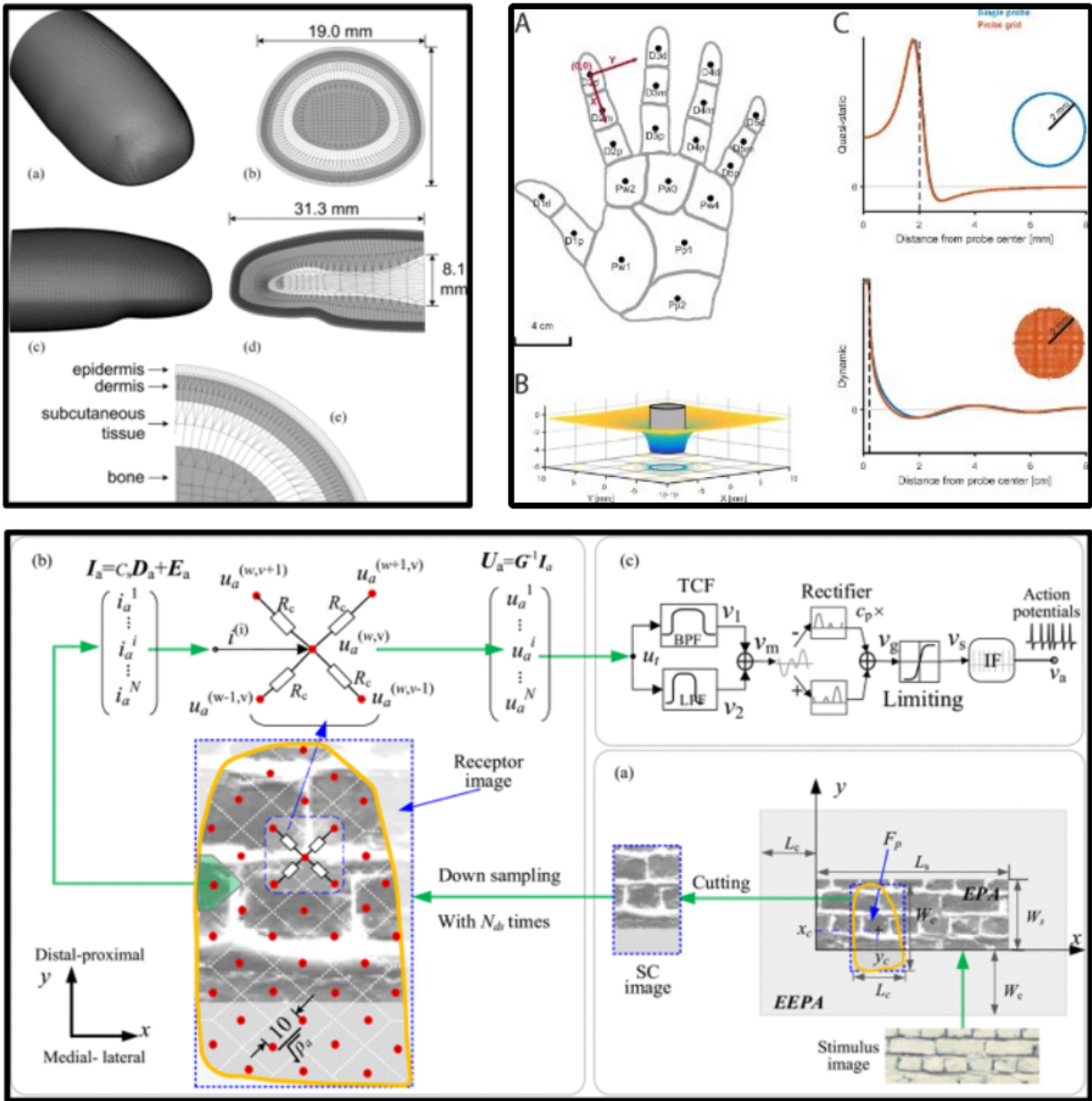


Figure 1.4: Right: FEM model [32]. Mechanoreceptor models available in the literature. Left: TouchSim continuum mechanics model [60]. Bottom: Resistor network model [53].

Chapter 2

Dynamic Modulation of Shear Shock Waves in Tissue to Advance Spatial Precision in Ultrasound Haptics

2.1 Introduction

The increased desire for innovative and effective ways to produce sensation in the human skin has led to the development of many different haptics technologies. Among the many developing technologies including glove-based vibrational haptic feedback devices, haptic chairs, vests, and suits [5, 16, 44, 50] are newer non-contact mid-air haptic systems. Mid-air haptic sensations can be elicited through various means such as with air jets [65], electromagnetic fields [72], and more prominently focused ultrasound [41]. Holographic mid-air haptics using ultrasound provides a new avenue for contactless sensations, which has applications in virtual reality, surgical training/simulations, the automobile industry, and assistive devices for the sensorially impaired.

Ultrasound waves are pressure waves that oscillate at frequencies above the audible human hearing range (~ 20 kHz). Ultrasound-facilitated haptic sensations first begin with a small focused region of acoustic pressure. Focused ultrasound has many medical applications such

as targeted drug delivery [21], tumor ablation [75], and neuromodulation [51]. Ultrasound waves incident on an object with a high impedance mismatch relative to air are reflected, resulting in a pressure exerted on the surface. This pressure induces a nonlinear acoustic radiation force, inducing deflections on the skin [15].

When focused ultrasound is used to trigger frequencies within the perceptible range, nerve endings known as mechanoreceptors, located in the dermal layer of the human skin, can be excited from skin deflections to produce sensational information that is sent to the brain, similar to a physical touch occurring on the surface of the skin.

The primary somatosensory groups which are effectively excited via mid-air haptics include the Meissner and Pacinian corpuscle mechanoreceptor groups. Meissner corpuscles are classified as rapidly adapting type 1 receptors (FA1), and can sense changes in skin deformation at a frequency range of 5-300 Hz. The Meissner group is located in the upper layer of the dermis, close to the dermal-epidermal boundary. Pacinian corpuscles, on the other hand, are classified as rapidly adapting type 2 receptors (FA2), and are typically located deeper in the dermal layer (up to 4mm). FA2 receptors can sense deformation changes in a frequency range of 5-800 Hz [23]. Typical models related to mid-air haptics are conducted with the assumption that the type of skin present is glabrous (hairless) and has a flat surface, which mostly approximates the palm. Other subtleties such as papillary and dermal ridges are often not considered.

Focused ultrasound may be generated through various methods. Phased array transducers (PATs) are devices which consist of an array of equally spaced ultrasound transducers, often in the form of a rectangular 2D grid. PATs are able to generate focal regions at a desired target plane by precisely controlling the phase and/or amplitude of the ultrasound waves in real time [2, 52, 67]. Although PATs offer robust real-time control over the emitted waves, their spatial resolution is a significant limitation, as achieving high resolution requires diffraction-

limited, small piezoelectric elements, which are costly to produce. Acoustic holographic lenses (AHLs), on the other hand, are engineered metasurfaces that offer higher spatial resolution at a lower cost [8, 47, 63], but their static acoustic fields make them challenging to apply in ultrasound haptics.

Upon the initial application of focused ultrasound, low-frequency components are generated from the initial skin impact/deflection caused by the nonlinear acoustic radiation force. However, after a short duration, the stable ultrasound focus point becomes imperceptible, as its frequency lies outside the human perceptible range [31]. Amplitude modulation (AM) is a commonly used technique to generate sensation in the skin by modulating the higher, un-sensed frequency signal to a lower-frequency amplitude envelope which can be sensed [54]. Although AM reduces the power and intensity received by the skin, thereby decreasing the intensity of the sensation, it remains effective in initiating the sensations in the first place. Lateral modulation (LM) or spatiotemporal modulation (STM), on the other hand, may be used to generate sensation in a moving trajectory focal point, this occurs by exciting nonlinear radiation force effects along the trajectory. Unlike AM for 2D shapes, LM and STM concentrate the PAT power into a single focal point, maximizing the intensity at that location. The main difference between lateral and spatiotemporal modulation, is that spatiotemporal modulation is not restricted to a lateral or straight-line motion, but instead can consist of any shape.

Surface wave propagation on the skin typically averages around 5 m/s, and when STM is applied at higher scanning speeds, users report distinct changes in tactile sensation, particularly in terms of perceived intensity and spatial localization. Frier et al. demonstrated that the maximum tactile response strength from STM is achieved when the focal point speed is in the range of 5–8 m/s. They attributed this effect to spatial summation occurring when the focal point speed reaches or exceeds the surface wave speed of the skin [27]. Reardon

et al. further investigated the STM with variable scanning speeds and demonstrated that the formation of shear shock waves results in poor localization of the tactile sensation at the focal point [57].

Several studies have aimed to develop hybrid modulation techniques capable of facilitating dynamic stimulation for an improved tactile experience. Rutten et al. investigated the perception of various shapes and found that the dynamic movement of a single amplitude-modulated point along the perimeter of the shape is perceived more effectively than multiple static points [59]. Hajas et al. reached a similar conclusion by proposing a combined method using amplitude modulation (AM) and spatiotemporal modulation (STM), referred to as the dynamic tactile pointer (DTP) [35]. They found that this method effectively localized the shape's edges by reducing the scanning speeds around the corners. Although enhanced tactile sensation has been observed in many cases under dynamic stimulation, a comprehensive analysis of the underlying physical mechanisms remains lacking, limiting interpretability.

A common issue with applying LM and STM with speeds higher than the surface wave speed of the tissue is the poor localization of the sensed focal point along the trajectory. Several user feedback studies have reported difficulty in accurately localizing the focus point [15, 57]. Although much of the current research primarily focuses on user experiences, the underlying physics of wave mechanics on the skin is undoubtedly important. Reardon et al. showed that the poor localization arises from the formation of shear shock waves due to constructive interference when the lateral modulation speed exceeds the shear wave speed in the skin [57]. The conical shape of the shock waves results in high-intensity regions extending several orders of magnitude beyond the focal point. In this work, an in-depth analysis of several techniques, including the integration of two modulation methods, is conducted to investigate their effects on the intensity and localization of the waves. Additionally, a variable modulation speed was employed to mitigate the constructive interference and formation of shock waves.

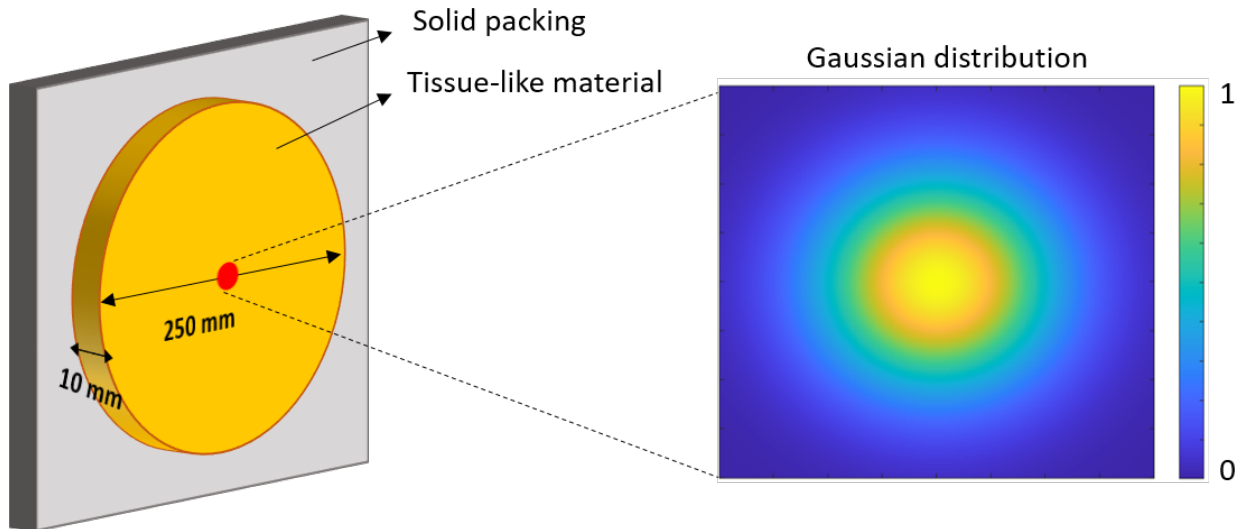


Figure 2.1: A schematic representation of the system, including a backing material, illustrating the focal point characterized by a Gaussian distribution with a variable full width at half maximum (FWHM).

2.2 System Model

There are different techniques used to simulate the wave propagation in the time domain. Finite Element Modeling (FEM) represents a common method used. FEM typically requires a mesh size of $\lambda/10$ or smaller for accurate calculation of the field, with the exact requirement depending on whether the system is linear, heterogeneous, or has complex geometry. The k-wave pseudospectral method has relaxed spatial meshing requirements, making it more efficient for simulating complex 3D problems compared to the FEM method. As opposed to FEM, the pseudospectral method computes spatial derivatives using Fourier-based techniques. This spectral accuracy allows for fewer required grid points in the mesh (when compared to FEM), given that the sampling meets the Nyquist criterion (at least two points per wavelength). It is important to note that for nonlinear problems, a mesh convergence analysis is essential to ensure an accurate solution, especially with FEM. In this work, we use the k-wave pseudospectral method implemented in MATLAB with a mesh size of $\lambda/3$.

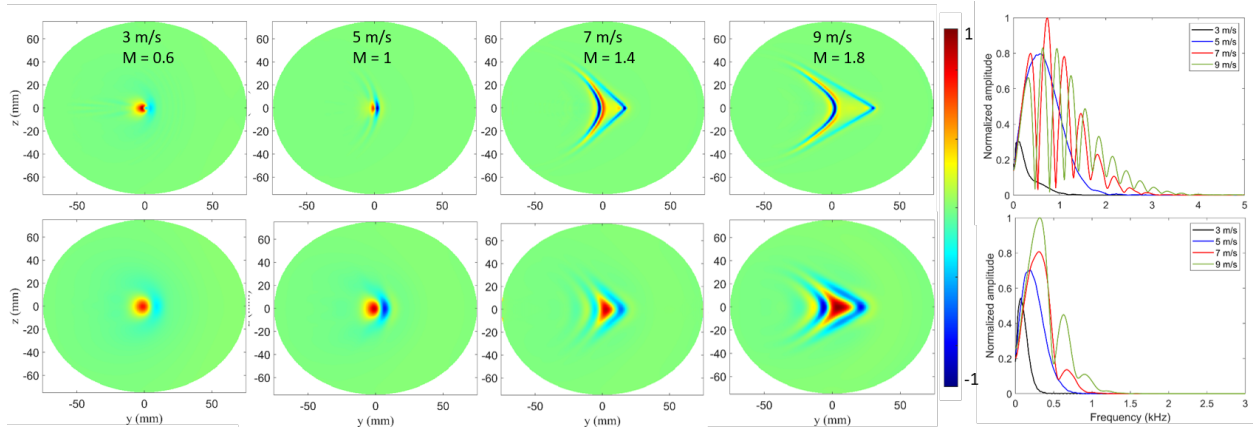


Figure 2.2: k-Wave simulation results of the out-of-plane displacement of the tissue-like material for different focal point scanning speeds. The ultrasound focal point is modeled as a displacement boundary with a spatial Gaussian distribution, with FWHM values of 2 mm (upper row) and 6 mm (lower row). In the case of scanning of a 2 mm FWHM focal point at 7 m/s, the out-of-plane displacement is recorded to be in the range of $2.19 \mu\text{m}$ and $-3.34 \mu\text{m}$. A normalized color bar is used for comparison purposes across all scanning scenarios. The figure also includes the FFT results of the displacement at the center of the tissue-like material.

Figure 2.1 illustrates the system considered, with labeled components, implemented in MATLAB to solve for wave propagation using the k-wave pseudospectral method. A tissue-like material with a shear wave speed of 5 m/s is employed to simulate human skin and attached to a solid packing material. A moving-focus ultrasound point is used to excite the tissue-like material, represented by a 2D Gaussian distribution, as shown in Figure 2.1.

2.3 Results and Discussion

The k-Wave simulation results of the out-of-plane displacement on the surface of the tissue-like material are shown in Fig. 2.2. A spatiotemporal modulation (STM) technique is applied to the scanning focal point, which is modeled as a dynamic surface displacement boundary condition to enhance computational efficiency. A sinusoidal temporal function with a carrier frequency of 40 kHz is applied to the displacement at each point, while the Gaussian focal

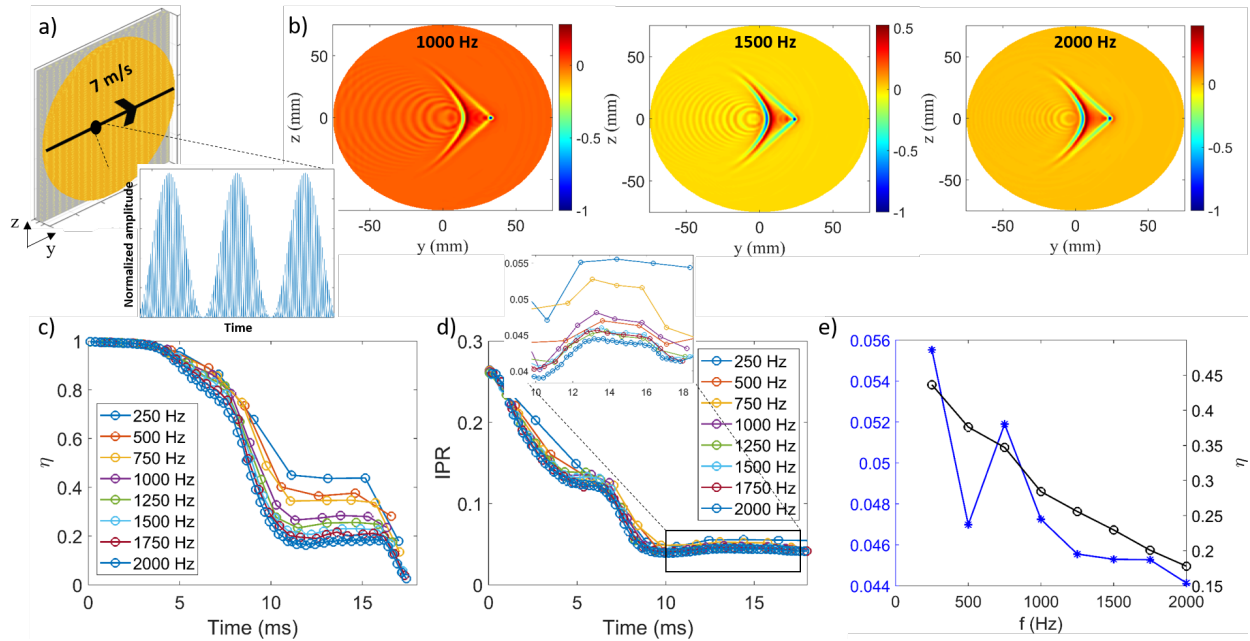


Figure 2.3: (a) A schematic of the system showing a moving focal point along a straight line, with the signal applied to the focal point being amplitude-modulated. (b) Normalized out-of-plane displacement of the tissue-like material surface at a fixed time, with the Gaussian point source swept along a linear path at a speed of 7 m/s; each plot corresponds to a different modulation frequency, with an ultrasound excitation carrier frequency of 40 kHz. (c) Reconstruction efficiency (η) as a function of simulation time, with the point source sweeping from left to right across the tissue-like material surface at different modulation frequencies. (d) Inverse participation ratio (IPR) as a function of simulation time. (e) The η and IPR values extracted at 14 ms (steady state) from (c) and (d) as a function of modulation frequency.

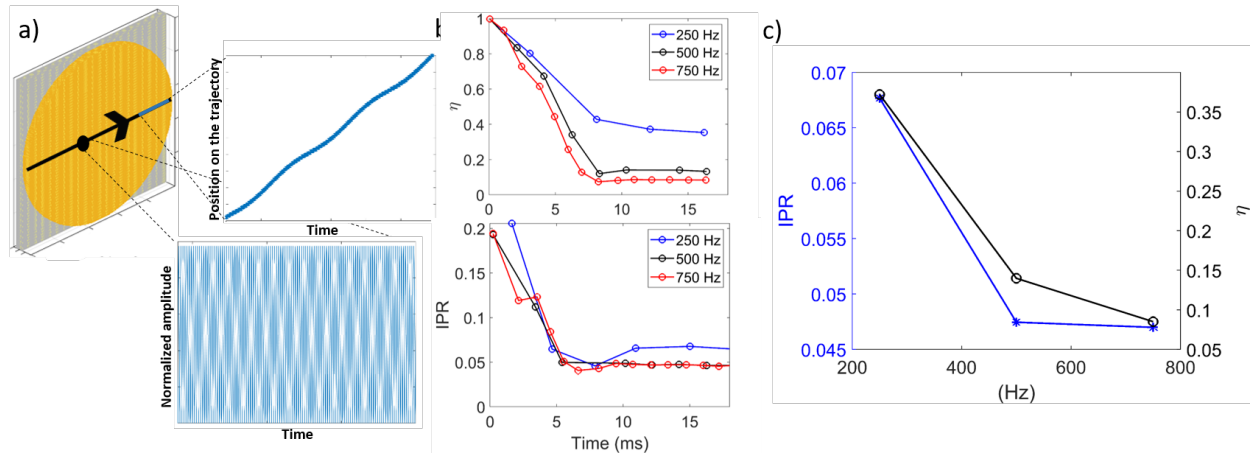


Figure 2.4: (a) A schematic of the system showing a moving focal point along a straight line, with the signal applied to the focal point, and the spatial position of the point as a function of time. (b) η and IPR as a function of simulation time, with the point source sweeping from left to right across the tissue-like material surface at different frequencies of speed oscillation. (d) The η and IPR values extracted at 14 ms (steady state) from (b) as a function of the frequency of speed oscillation.

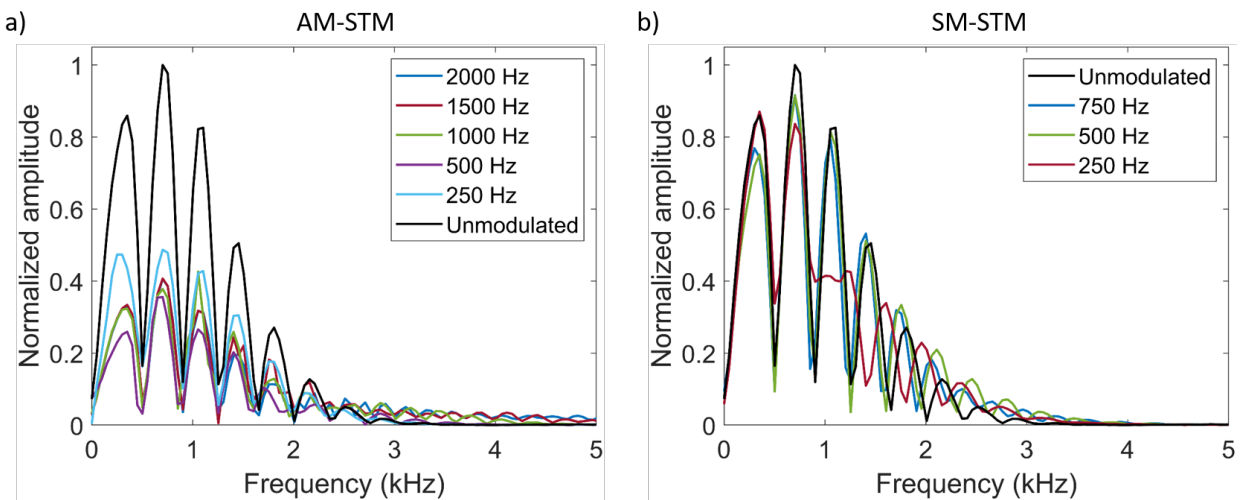


Figure 2.5: (a) FFT analysis of the out-of-plane displacement at the center of the tissue-like material using the AM-STM technique with a scanning speed of 7 m/s at different modulation frequencies. (b) Similar analysis for the SM-STM technique with a variable sinusoidal scanning speed, averaging 7 m/s, at different speed frequencies

point is swept in a straight line from left to right across the tissue-like material surface. The presented results in Fig. 2.2 illustrate the out-of-plane displacement at a specific time when the focal point reaches the center of the domain. The first row corresponds to simulations with a full width at half maximum (FWHM) of 2 mm and the second row corresponds to FWHM of 6 mm. For scanning speeds below the shear wave speed of the tissue-like material ($M < 1$), the displacement profile corresponds to a focal point moving along the trajectory. When the scanning speed exceeds the shear wave speed ($M > 1$), a shock wave forms, exhibiting a conical high-intensity structure due to constructive interference. An FFT analysis is performed for each simulation at varying scanning speeds. The FFT results reveal peaks at lower frequencies that vary with scanning speed. As the scanning speed increases, the dominant frequency also increases, as shown in Fig. 2.2. Despite the excitation frequency being set to 40 kHz, low-frequency components are generated due to the nonlinear radiation force [57]. The FFT results for all scanning speeds show high amplitude in the 100-500 Hz range for a FWHM of 6 mm, and in the 100-1000 Hz range for a FWHM of 2 mm. It is well-established that human tactile sensitivity generally peaks around 200-250 Hz, which mainly target Meissner and Pacinian corpuscles [45]. These same rapidly-adapting afferent types can also sense other low frequencies (> 1000), where the strength of the sensation may rely on factors such as spatial resolution and indentation depth. This indicates that the low frequency components generated by STM are effective in eliciting sensations at different scanning speeds. This also demonstrates that the excited frequency can be effectively controlled by adjusting the FWHM of the focal point and its scanning speed. Although using STM with higher scanning speeds (5-8 m/s) increases the overall field intensity through constructive interference and cone formation (wavefront summation effect) [27], the energy is distributed over a larger area, resulting in reduced localization [57]. The AM-STM method is applied to a focal point that is swept along a straight line, as

depicted in Fig. 2.3 (a). The focal point is approximated by a Gaussian displacement point moving at a velocity of 7 m/s. The signal is shifted above the x-axis to induce positive displacement, and an envelope function is applied with a minimum amplitude of zero and a maximum amplitude of one. The out-of-plane displacement results of the tissue-like material surface at a fixed time, obtained from k-wave simulations, are shown in Fig. 2.3 (b) for different modulation frequencies. Due to the Mach number of the moving point exceeding 1 (specifically >1.4 when the shear speed is 5 m/s), all results indicate the formation of a shear shock wave with a conical geometry, where the waves undergo constructive interference. At first glance, the results may appear identical; however, the intensity of the cone relative to the focal point varies across all modulation frequencies. To quantify this, two metrics are employed: reconstruction efficiency (η) and inverse participation ratio (IPR). The reconstruction efficiency (η) serves as a measure of wake intensity and is defined as the ratio of the out-of-plane displacement at the focal region to the displacement elsewhere in the field and is mathematically represented as $\eta = \sum u_{\text{focal}}^2(x, y, Z_t) / \sum u^2(x, y, Z_t)$. The IPR serves as a measure of the localization of the displacement amplitude and is mathematically represented as $IPR = (\sum_i u_i)^2 / \sum_i u_i^2$ where u is the out-of-plane displacement on the tissue-like material surface. Figure 2.3 (c) illustrates the reconstruction efficiency (η) for various modulation frequencies. At 0 ms, $\eta = 1$ for all frequencies, as no shock has yet formed and the result solely reflects the focal point. After 10 ms, the system reaches a steady state for all modulation frequencies. It is observed that η consistently decreases with an increase in modulation frequency. Notably, this decrease asymptotically approaches the value observed in the spatiotemporal modulation (STM) case with no amplitude modulation (AM). Although η is a valuable metric for providing information about the ratio of focal to overall intensity, it does not convey information regarding the dispersion of the field, particularly around the focal point. The IPR results, shown in Fig. 2.3 (d), reveal only a slight change in localization as a function of the modulation frequency. To better visualize

the relationship between both metrics and the modulation frequency, η and IPR values are extracted at 14 ms (at the steady state region) and plotted in Fig. 2.3 (e). It is observed that there is nearly a linear inverse relationship between η and the modulation frequency, with the IPR values also plotted on the left axis.

The AM-STM method demonstrated effective reduction of wake intensity relative to the focal point intensity. However, AM reduces the output power relative to its modulation frequency, leading to a decrease in overall tactile sensation, which constitutes a limitation of applying AM. We propose a variable-scanning speed modulation STM mixed method (SM-STM) that facilitates less shock cone formation. Figure 2.4 (a) illustrates the system considered along with the point trajectory with a uniform input signal (no AM). The scanning speed oscillates sinusoidally between 5 and 9 m/s at a specified frequency, resulting in periodic acceleration and deceleration of the point along the trajectory. Figure 2.4 (a) illustrates the corresponding position along a segment of the trajectory, derived by integrating the speed. By varying the frequency of the speed oscillations, the intensity of the shock cone changes. Figure 2.4 shows the η values as a function of time when the point is scanned across the tissue-like material at different scanning frequencies. Figure 2.4 (b) depicts η and IPR as functions of time along the trajectory. It is observed that an increase in the frequency of the speed oscillations results in a decrease in both η and IPR values. This trend is evident by extracting the values at 14 ms (steady state), as shown in Figure 2.4 (c). This behavior can be attributed to the fact that shock formation requires a certain settling time to reach a steady state. By reducing the speed to Mach = 1 or below at specific intervals, the shock weakens, and when the speed increases again, there is insufficient time for the shock cone to fully form. Consequently, this leads to a higher η and IPR, indicating improved energy localization.

It is also crucial to study the amplitude of the sensible low-frequency signals generated on the tissue-like material. In Fig. 2.5, an FFT analysis of both the AM-STM and SM-STM

techniques is performed and normalized. The results show low-frequency generation within a similar range of 200-1500 Hz for both techniques. This can be attributed to the fact that, for both methods, the energy is spatially distributed uniformly with a FWHM of 3 mm. However, the FFT for the AM-STM technique, shown in Fig. 2.5 (a), demonstrates a reduction in amplitude compared to the unmodulated case, which is expected as modulating the signal reduces the output power applied to the tissue-like material, as previously noted. In contrast, the SM-STM technique exhibits a more significant improvement by maintaining a nearly constant amplitude while enhancing localization as shown in 2.5 (b), making it a highly promising technique for a wide range of applications.

TouchSim

TouchSim is a toolbox developed by Saal et al. [60] which models the response characteristics of mechanoreceptors in the human palm to a user-defined physical stimulus. This open-source simulation tool is compatible with both MATLAB and Python and may be used to predict the neural response of mechanical inputs to the palm surface. This two-stage model is divided into a continuum mechanics model for the mechanical input, and an integrate-and-fire neural model for the mechanoreceptor response. The continuum mechanics (CM) model analytically solves for both the quasistatic and dynamic/propagated stresses in the palm by relating the given indentation depth to a force using Hooke's Law. For the quasistatic component, the indentation depth is directly available from the user input. However, the dynamic component is calculated by propagating surface waves from the input pin at an 8 m/s speed of sound and a decay rate of $1/\text{pin radius}$. Also, the stiffness coefficient, k , is replaced by a viscous coefficient, c . In this model, the palm is assumed to be a frictionless elastic half-space, and is considered flat, homogenous, and isotropic. The output of the CM model is fed into an integrate-and-fire (IF) model to generate spike responses. The IF model includes 13

parameters which are multiplied by different weights and summed to a “potential”. When the potential hits one, a spike is triggered, and the potential is reset. The 13 parameters are as follows. First, a low-pass filter is applied, since mechanoreceptors naturally cannot sense frequencies above a certain value. The next six parameters are related to the calculated stress components: quasistatic, dynamic, and differentiated-dynamic. These components are separated into both positive and negative components and make up parameters 2-7, and are then summed. The following parameter is a saturating nonlinearity, which reflects mechanoreceptors’ natural tendency to saturate at high intensities (8), followed by Gaussian noise (9). The final three input parameters relate to a decaying time constant for the membrane potential, postspike inhibition, and an input time delay (10-13).

The results of two haptic scenarios are displayed in figures 2.6 and 2.7. In both scenarios, The PC afferent population is modeled alone, as it is the primary mechanoreceptor group of interest for higher-frequency inputs, at least in regards to typical frequencies applied in ultrasound haptics. Figure 2.6 displays a comparison between both a modulated (2.6b) and unmodulated (2.6a) stationary input. In the unmodulated case (2.6a), the 40 kHz signal is applied to the center of the palm for 1 second, and the predicted result is shown. Consistent with the literature and physics, it is shown that an initial firing of many spikes throughout the whole palm occurs. However, this only lasts for a short period of time ($> 0.015s$), and quickly stops since signals at extremely high frequencies cannot be felt. On the other hand, (2.6b) displays the result of a stationary input signal which is amplitude modulated with an envelope frequency of 200 Hz. As expected, since 200 Hz can be sensed by the PC afferent group, it is instead shown that there is a consistent firing rate of neurons in the localized area for the entire 1 second duration.

Figure 2.7 displays the result of an approximation for the spatiotemporal modulated scenario. While TouchSim doesn’t have the capability of fully modeling moving/scanning inputs, due

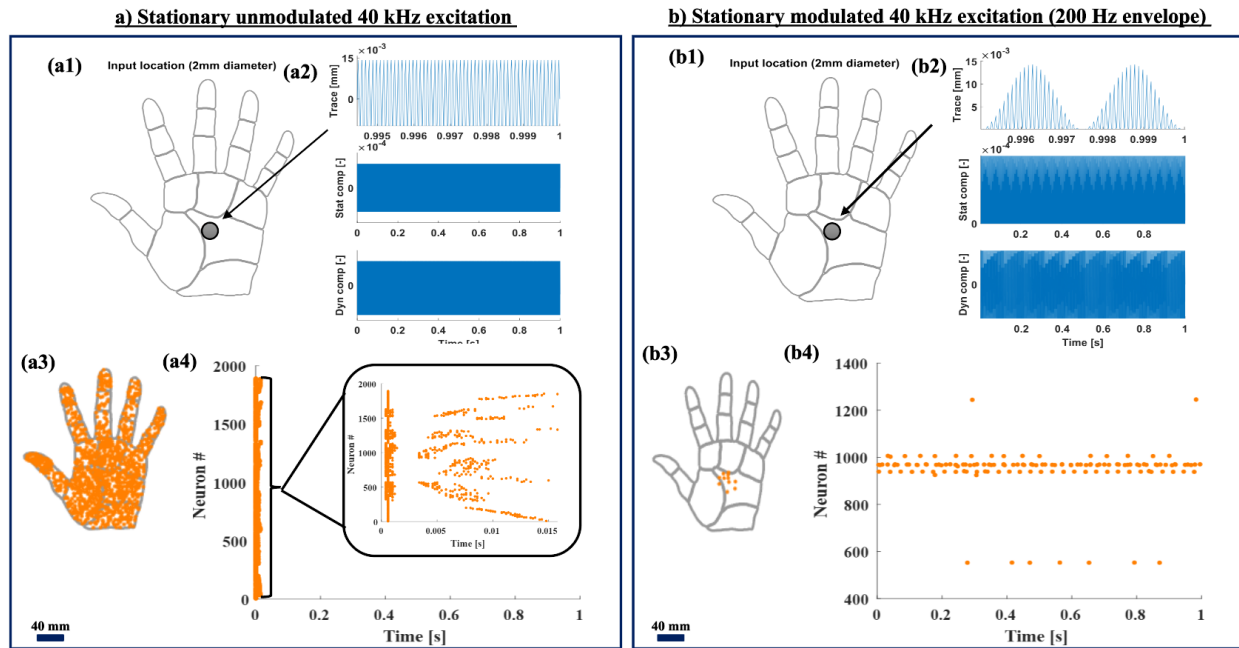


Figure 2.6: (a1,a2) A schematic of a 40 kHz input signal applied as a pin indentation to the center of the palm, marked by a large gray circle, which has a 2mm diameter (not shown to scale). (a3) Spatial representation of fired PC afferents, displaying the location of where receptors were activated throughout the hand. (a4) Spike raster plot which shows the neurons which are fired in the palm with respect to time. A zoomed-in image of the graph displays greater detail of the temporal spread of activated receptors, since all of the receptors are fired within the first 0.015 seconds. (b1,b2) Similar to 2.6a, a schematic is shown of a 200 Hz AM input signal applied as a pin indentation to the center of the palm, marked by a large gray circle, which has a 2mm diameter (not shown to scale). (b3) Spatial representation of fired PC afferents, displaying the location of where receptors were activated throughout the hand. (b4) Spike raster plot which shows the neurons which are fired in the palm with respect to time. In this scenario, it is shown that neurons are fired throughout the entire duration of the input signal.

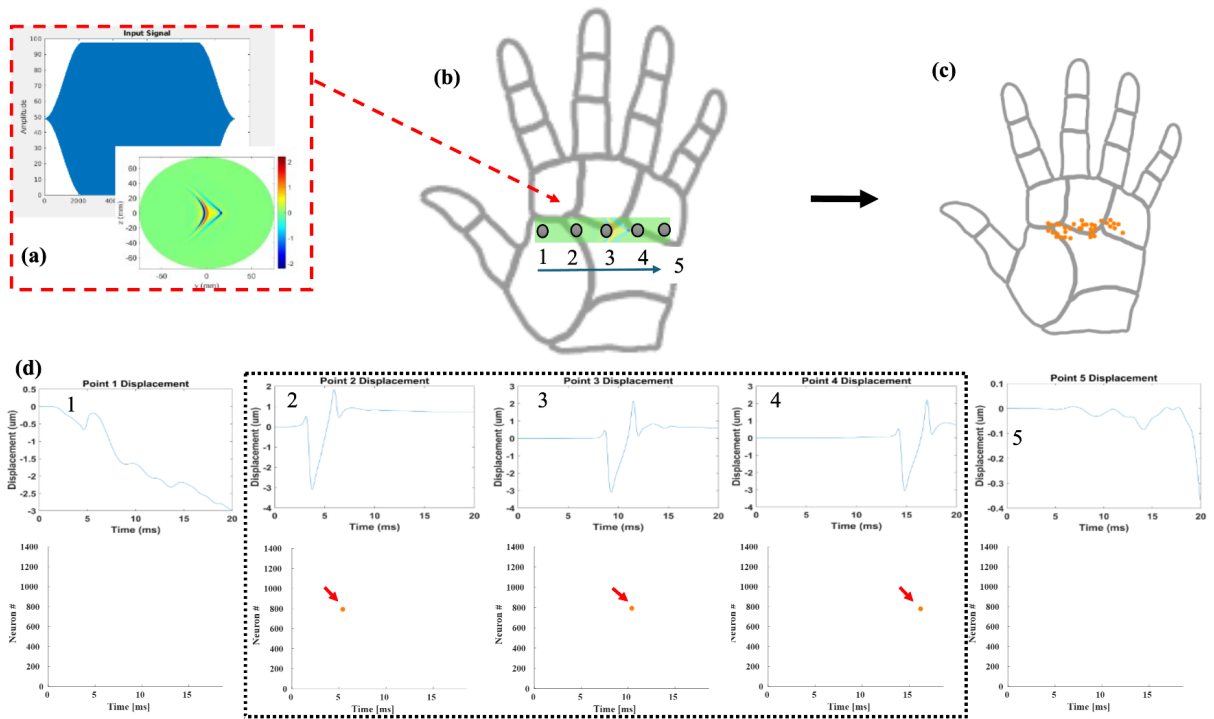


Figure 2.7: (a) The desired input signal for STM which is obtained from k-Wave simulations. (b) General location of the scanned input signal along the palm. Gray circles which are numbered 1-5 represent locations where neural response data was recorded/observed. (c) Spatial representation of fired neurons on the surface of the palm. (d) Plots relating to the input displacement (top) and neural response (bottom) at the 5 mentioned locations in 2.7b. A clear time delay in neuron firing can be seen in plots 2-4, which is expected for the moving points which reaches the consecutive locations after a certain time.

to the assumption of a frictionless surface, among other reasons, the neural response may still be generally approximated for comparative purposes using this toolbox, and is done so in its associated paper [60]. In order to approximate the scanning response for a constant intensity STM input, the time domain mechanical responses at each point of the k-Wave elastic simulation were extracted and inputted into TouchSim as perpendicular skin displacements. This provides a sufficient approximation, as the perpendicular displacement of the skin is the most primary contributor to mechanoreceptor activation. The resultant spatial plot (2.7c) indicates a general firing of receptors along the desired trajectory, as well as the time-delayed firing of neurons as the focal point is scanned across (2.7d). These results show significant potential for the use of TouchSim to predict the neural response of various ultrasound haptics scenarios, including but not limited to the modulation techniques conceptualized in this thesis.

2.4 Conclusion

The proposed mixed amplitude and spatiotemporal modulation (AM-STM) and variable scanning speed modulation (SM-STM) techniques offer promising advancements in non-contact ultrasound haptics. While traditional methods often struggle with a trade-off between intensity and localization, the presented techniques effectively address these challenges. The AM-STM approach successfully reduces the wake effect, although it comes with a decrease in intensity. On the other hand, the SM-STM technique enhances localization with minimal impact on intensity, offering a more promising solution to the tactile localization. These findings highlight the potential for these methods to improve tactile feedback in a range of applications, paving the way for more precise and efficient ultrasound haptic systems. TouchSim results also display the potential for ultrasound haptics researchers to further understand the neural mechanisms which contribute to sensation.

Bibliography

- [1] Moaed A Abd, Joseph Ingicco, Douglas T Hutchinson, Emmanuelle Tognoli, and Erik D Engeberg. Multichannel haptic feedback unlocks prosthetic hand dexterity. *Scientific reports*, 12(1):2323, 2022.
- [2] Rais Ahmad, Tribikram Kundu, and Dominique Placko. Modeling of phased array transducers. *The Journal of the Acoustical Society of America*, 117(4):1762–1776, 2005.
- [3] Moustafa Sayed Ahmed and Shima Shahab. Dynamic and reconfigurable acoustic fields enabled by morphing fluidic holographic lenses. *ADVANCED MATERIALS TECHNOLOGIES*, 2025.
- [4] Moustafa Sayed Ahmed and Shima Shahab. Wave-field shaping with elastic metasurfaces via the iterative angular-spectrum approach. *Physical Review Applied*, 23(5):054056, 2025.
- [5] Víctor H Andaluz, Edgar F Borja, Daniel A Lara, and Pablo A Zambrano. Vibrating haptic stimulation glove for virtual reality environments. *Advanced Science Letters*, 24(11):8841–8845, 2018.
- [6] Haim Azhari. *Appendix A: Typical Acoustic Properties of Tissues*, pages 313–314. 2010. doi: 10.1002/9780470561478.app1.
- [7] Haim Azhari. *Ultrasonic Waves in Fluids*, pages 55–73. 2010. doi: 10.1002/9780470561478.ch3.
- [8] Marjan Bakhtiari-Nejad, Ahmed Elnahhas, Muhammad R Hajj, and Shima Shahab.

- Acoustic holograms in contactless ultrasonic power transfer systems: Modeling and experiment. *Journal of Applied Physics*, 124(24), 2018.
- [9] Marjan Bakhtiari-Nejad, Muhammad R Hajj, and Shima Shahab. Dynamics of acoustic impedance matching layers in contactless ultrasonic power transfer systems. *Smart Materials and Structures*, 29(3):035037, 2020.
- [10] Mark F. Bear, Barry W. Connors, and Michael A. Paradiso. Neuroscience: Exploring the brain, 3rd ed. 2007. URL <https://api.semanticscholar.org/CorpusID:149872724>.
- [11] Aarushi Bhargava, Vamsi C Meesala, Muhammad R Hajj, and Shima Shahab. Nonlinear effects in high-intensity focused ultrasound power transfer systems. *Applied Physics Letters*, 117(6), 2020.
- [12] Stanley J Bolanowski Jr, George A Gescheider, Ronald T Verrillo, and Christin M Checkosky. Four channels mediate the mechanical aspects of touch. *The Journal of the Acoustical society of America*, 84(5):1680–1694, 1988.
- [13] Edgar F. Borja, Daniel A. Lara, Washington X. Quevedo, and Víctor H. Andaluz. Haptic stimulation glove for fine motor rehabilitation in virtual reality environments. In Lucio Tommaso De Paolis and Patrick Bourdot, editors, *Augmented Reality, Virtual Reality, and Computer Graphics*, pages 211–229, Cham, 2018. Springer International Publishing. ISBN 978-3-319-95282-6.
- [14] Stefan Josef Breitschaft, Stella Clarke, and Claus-Christian Carbon. A theoretical framework of haptic processing in automotive user interfaces and its implications on design and engineering. *Frontiers in psychology*, 10:1470, 2019.
- [15] Tom Carter, Sue Ann Seah, Benjamin Long, Bruce Drinkwater, and Sriram Subramanian. Ultrahaptics: multi-point mid-air haptic feedback for touch surfaces. In

- Proceedings of the 26th Annual ACM Symposium on User Interface Software and Technology*, UIST '13, page 505–514, New York, NY, USA, 2013. Association for Computing Machinery. ISBN 9781450322683. doi: 10.1145/2501988.2502018. URL <https://doi.org/10.1145/2501988.2502018>.
- [16] Bora Celebi, Müge Cavdan, and Knut Drewing. Design and evaluation of a multimodal haptic vest. In *2023 IEEE World Haptics Conference (WHC)*, pages 56–63, 2023. doi: 10.1109/WHC56415.2023.10224374.
- [17] Ceren Cengiz and Shima Shahab. Holographic thermal mapping in volumes using acoustic lenses. *Journal of Physics D: Applied Physics*, 57(36):365501, 2024.
- [18] Ceren Cengiz, Zekeriya Ender Eger, Mihir Pewekar, Pinar Acar, Wynn Legon, and Shima Shahab. A roadmap to holographic focused ultrasound approaches for generating gradient thermal patterns. *International Journal for Numerical Methods in Biomedical Engineering*, 41(6):e70055, 2025.
- [19] CH Chaussy, Walter Brendel, and E Schmiedt. Extracorporeally induced destruction of kidney stones by shock waves. *The Lancet*, 316(8207):1265–1268, 1980.
- [20] Jamie Chilles, William Frier, Abdenaceur Abdouni, Marcello Giordano, and Orestis Georgiou. Laser doppler vibrometry and fem simulations of ultrasonic mid-air haptics. In *2019 IEEE World Haptics Conference (WHC)*, pages 259–264, 2019. doi: 10.1109/WHC.2019.8816097.
- [21] Constantin C Coussios and Ronald A Roy. Applications of acoustics and cavitation to noninvasive therapy and drug delivery. *Annu. Rev. Fluid Mech.*, 40(1):395–420, 2008.
- [22] Diane Dalecki, Sally Z Child, Carol H Raeman, and Edwin L Carstensen. Tactile

- perception of ultrasound. *The Journal of the Acoustical Society of America*, 97(5): 3165–3170, 1995.
- [23] Davide Deflorio, Massimiliano Di Luca, and Alan M Wing. Skin and mechanoreceptor contribution to tactile input for perception: a review of simulation models. *Frontiers in Human Neuroscience*, 16:862344, 2022.
- [24] Nguyen Minh Duc and Bilgin Keserci. Emerging clinical applications of high-intensity focused ultrasound. *Diagnostic and Interventional Radiology*, 25(5):398, 2019.
- [25] Alejandro Flores Ramones and Marta Sylvia del Rio-Guerra. Recent developments in haptic devices designed for hearing-impaired people: A literature review. *Sensors*, 23(6):2968, 2023.
- [26] William Frier, Damien Ablart, Jamie Chilles, Benjamin Long, Marcello Giordano, Marianna Obrist, and Sriram Subramanian. Using spatiotemporal modulation to draw tactile patterns in mid-air. In Domenico Prattichizzo, Hiroyuki Shinoda, Hong Z. Tan, Emanuele Ruffaldi, and Antonio Frisoli, editors, *Haptics: Science, Technology, and Applications*, pages 270–281, Cham, 2018. Springer International Publishing. ISBN 978-3-319-93445-7.
- [27] William Frier, Damien Ablart, Jamie Chilles, Benjamin Long, Marcello Giordano, Marianna Obrist, and Sriram Subramanian. Using spatiotemporal modulation to draw tactile patterns in mid-air. In *Haptics: Science, Technology, and Applications: 11th International Conference, EuroHaptics 2018, Pisa, Italy, June 13-16, 2018, Proceedings, Part I 11*, pages 270–281. Springer, 2018.
- [28] Penghao Gao, Yue Sun, Gongsen Zhang, Chunsheng Li, and Linlin Wang. A transducer positioning method for transcranial focused ultrasound treatment of brain tumors. *Frontiers in Neuroscience*, 17:1277906, 2023.

- [29] Leonid R. Gavrilov, Grigoryi V. Gersuni, Oleg B. Ilyinski, Efim M. Tsirolnikov, and Eugenyi E. Shchekanov. A study of reception with the use of focused ultrasound. i. effects on the skin and deep receptor structures in man. *Brain Research*, 135(2):265–277, 1977. ISSN 0006-8993. doi: [https://doi.org/10.1016/0006-8993\(77\)91030-7](https://doi.org/10.1016/0006-8993(77)91030-7). URL <https://www.sciencedirect.com/science/article/pii/0006899377910307>.
- [30] Leonid R. Gavrilov, Grigoryi V. Gersuni, Oleg B. Ilyinsky, Efim M. Tsirolnikov, and Eugenyi E. Shchekanov. A study of reception with the use of focused ultrasound. ii. effects on the animal receptor structures. *Brain Research*, 135(2):279–285, 1977. ISSN 0006-8993. doi: [https://doi.org/10.1016/0006-8993\(77\)91031-9](https://doi.org/10.1016/0006-8993(77)91031-9). URL <https://www.sciencedirect.com/science/article/pii/0006899377910319>.
- [31] Orestis Georgiou, William Frier, Euan Freeman, Claudio Pacchierotti, and Takayuki Hoshi. *Ultrasound mid-air haptics for touchless interfaces*, volume 3. Springer, 2022.
- [32] Gregory J Gerling, Isabelle I Rivest, Daine R Lesniak, Jacob R Scanlon, and Lingtian Wan. Validating a population model of tactile mechanotransduction of slowly adapting type i afferents at levels of skin mechanics, single-unit response and psychophysics. *IEEE transactions on haptics*, 7(2):216–228, 2013.
- [33] D. Gomez, G. Burdea, and N. Langrana. Integration of the rutgers master ii in a virtual reality simulation. In *Proceedings of the Virtual Reality Annual International Symposium (VRAIS'95)*, VRAIS '95, page 198, USA, 1995. IEEE Computer Society. ISBN 0818670843.
- [34] Johannes Gruetzmacher. Piezoelektrischer kristall mit ultraschallkonvergenz. *Zeitschrift für Physik*, 96(5):342–349, 1935.
- [35] Daniel Hajas, Dario Pittera, Antony Nasce, Orestis Georgiou, and Marianna Obrist.

- Mid-air haptic rendering of 2d geometric shapes with a dynamic tactile pointer. *IEEE Transactions on Haptics*, 13(4):806–817, 2020. doi: 10.1109/TOH.2020.2966445.
- [36] Keisuke Hasegawa and Hiroyuki Shinoda. *Modulation Methods for Ultrasound Midair Haptics*, pages 225–240. Springer International Publishing, Cham, 2022. ISBN 978-3-031-04043-6. doi: 10.1007/978-3-031-04043-6_9. URL https://doi.org/10.1007/978-3-031-04043-6_9.
- [37] Takayuki Hoshi and Hiroyuki Shinoda. *Airborne Ultrasound Tactile Display*, pages 121–138. Springer Japan, Tokyo, 2016. ISBN 978-4-431-55772-2. doi: 10.1007/978-4-431-55772-2_8. URL https://doi.org/10.1007/978-4-431-55772-2_8.
- [38] Takayuki Hoshi, Takayuki Iwamoto, and Hiroyuki Shinoda. Non-contact tactile sensation synthesized by ultrasound transducers. In *World Haptics 2009 - Third Joint EuroHaptics conference and Symposium on Haptic Interfaces for Virtual Environment and Teleoperator Systems*, pages 256–260, 2009. doi: 10.1109/WHC.2009.4810900.
- [39] Takayuki Hoshi, Masafumi Takahashi, Takayuki Iwamoto, and Hiroyuki Shinoda. Non-contact tactile display based on radiation pressure of airborne ultrasound. *IEEE Transactions on Haptics*, 3(3):155–165, 2010. doi: 10.1109/TOH.2010.4.
- [40] Takayuki Iwamoto, Mari Tatezono, Takayuki Hoshi, and Hiroyuki Shinoda. Airborne ultrasound tactile display. In *ACM SIGGRAPH 2008 New Tech Demos*, SIGGRAPH '08, New York, NY, USA, 2008. Association for Computing Machinery. ISBN 9781450378475. doi: 10.1145/1401615.1401616. URL <https://doi.org/10.1145/1401615.1401616>.
- [41] Takayuki Iwamoto, Mari Tatezono, and Hiroyuki Shinoda. Non-contact method for producing tactile sensation using airborne ultrasound. In Manuel Ferre, editor, *Haptics:*

- Perception, Devices and Scenarios*, pages 504–513, Berlin, Heidelberg, 2008. Springer Berlin Heidelberg. ISBN 978-3-540-69057-3.
- [42] D. Jack, R. Boian, A.S. Merians, M. Tremaine, G.C. Burdea, S.V. Adamovich, M. Recce, and H. Poizner. Virtual reality-enhanced stroke rehabilitation. *IEEE Transactions on Neural Systems and Rehabilitation Engineering*, 9(3):308–318, 2001. doi: 10.1109/7333.948460.
- [43] Lawrence E Kinsler, Austin R Frey, Alan B Coppens, and James V Sanders. *Fundamentals of acoustics*. John wiley & sons, 2000.
- [44] Yukari Konishi, Nobuhisa Hanamitsu, Benjamin Outram, Kouta Minamizawa, Tetsuya Mizuguchi, and Ayahiko Sato. Synesthesia suit: the full body immersive experience. In *ACM SIGGRAPH 2016 VR Village*, SIGGRAPH '16, New York, NY, USA, 2016. Association for Computing Machinery. ISBN 9781450343770. doi: 10.1145/2929490.2932629. URL <https://doi.org/10.1145/2929490.2932629>.
- [45] Susan J Lederman and Roberta L Klatzky. Haptic perception: A tutorial. *Attention, Perception, & Psychophysics*, 71(7):1439–1459, 2009.
- [46] Zhichao Ma, Andrew W Holle, Kai Melde, Tian Qiu, Korbinian Poeppel, Vincent Mauricio Kadiri, and Peer Fischer. Acoustic holographic cell patterning in a biocompatible hydrogel. *Advanced Materials*, 32(4):1904181, 2020.
- [47] Kai Melde, Andrew G Mark, Tian Qiu, and Peer Fischer. Holograms for acoustics. *Nature*, 537(7621):518–522, 2016.
- [48] Kai Melde, Heiner Kremer, Minghui Shi, Senne Seneca, Christoph Frey, Ilia Platzman, Christian Degel, Daniel Schmitt, Bernhard Schölkopf, and Peer Fischer. Compact holographic sound fields enable rapid one-step assembly of matter in 3d. *Sci-*

- ence Advances*, 9(6):eadf6182, 2023. doi: 10.1126/sciadv.adf6182. URL <https://www.science.org/doi/abs/10.1126/sciadv.adf6182>.
- [49] Lendy Mulot, Thomas Howard, Claudio Pacchierotti, and Maud Marchal. Improving the perception of mid-air tactile shapes with spatio-temporally-modulated tactile pointers. *ACM Trans. Appl. Percept.*, 20(4), October 2023. ISSN 1544-3558. doi: 10.1145/3611388. URL <https://doi.org/10.1145/3611388>.
- [50] Suranga Nanayakkara, Elizabeth Taylor, Lonce Wyse, and S H. Ong. An enhanced musical experience for the deaf: design and evaluation of a music display and a haptic chair. In *Proceedings of the SIGCHI Conference on Human Factors in Computing Systems*, CHI '09, page 337–346, New York, NY, USA, 2009. Association for Computing Machinery. ISBN 9781605582467. doi: 10.1145/1518701.1518756. URL <https://doi.org/10.1145/1518701.1518756>.
- [51] Omer Naor, Steve Krupa, and Shy Shoham. Ultrasonic neuromodulation. *Journal of neural engineering*, 13(3):031003, 2016.
- [52] Yoichi Ochiai, Takayuki Hoshi, and Jun Rekimoto. Three-dimensional mid-air acoustic manipulation by ultrasonic phased arrays. *PloS one*, 9(5):e97590, 2014.
- [53] Qiangqiang Ouyang, Juan Wu, Zhiyu Shao, Dapeng Chen, and James W Bisley. A simplified model for simulating population responses of tactile afferents and receptors in the skin. *IEEE Transactions on Biomedical Engineering*, 68(2):556–567, 2020.
- [54] Gunhyuk Park and Seungmoon Choi. Perceptual space of amplitude-modulated vibrotactile stimuli. In *2011 IEEE world haptics conference*, pages 59–64. IEEE, 2011.
- [55] Pinyo Puangmali, Kaspar Althoefer, Lakmal D. Seneviratne, Declan Murphy, and

- Prokar Dasgupta. State-of-the-art in force and tactile sensing for minimally invasive surgery. *IEEE Sensors Journal*, 8(4):371–381, 2008. doi: 10.1109/JSEN.2008.917481.
- [56] Gregory Reardon, Bharat Dandu, Yitian Shao, and Yon Visell. Shear shock waves mediate haptic holography via focused ultrasound. *Science Advances*, 9(9):eadf2037, 2023. doi: 10.1126/sciadv.adf2037. URL <https://www.science.org/doi/abs/10.1126/sciadv.adf2037>.
- [57] Gregory Reardon, Bharat Dandu, Yitian Shao, and Yon Visell. Shear shock waves mediate haptic holography via focused ultrasound. *Science Advances*, 9(9):eadf2037, 2023.
- [58] Jun Rekimoto. Senseablerays: opto-haptic substitution for touch-enhanced interactive spaces. In *CHI '09 Extended Abstracts on Human Factors in Computing Systems*, CHI EA '09, page 2519–2528, New York, NY, USA, 2009. Association for Computing Machinery. ISBN 9781605582474. doi: 10.1145/1520340.1520356. URL <https://doi.org/10.1145/1520340.1520356>.
- [59] Isa Rutten, William Frier, Lawrence Van den Bogaert, and David Geerts. Invisible touch: How identifiable are mid-air haptic shapes? In *Extended abstracts of the 2019 CHI conference on human factors in computing systems*, pages 1–6, 2019.
- [60] Hannes P. Saal, Benoit P. Delhaye, Brandon C. Rayhaun, and Sliman J. Bensmaia. Simulating tactile signals from the whole hand with millisecond precision. *Proceedings of the National Academy of Sciences*, 114(28):E5693–E5702, 2017. doi: 10.1073/pnas.1704856114. URL <https://www.pnas.org/doi/abs/10.1073/pnas.1704856114>.
- [61] Ahmed Sallam and Shima Shahab. On nonlinear effects in holographic-modulated ultrasound. *Applied Physics Letters*, 121(20), 2022.

- [62] Ahmed Sallam and Shima Shahab. Nonlinear acoustic holography with adaptive sampling. *IEEE Transactions on Ultrasonics, Ferroelectrics, and Frequency Control*, 70(11):1516–1526, 2023. doi: 10.1109/TUFFC.2023.3315011.
- [63] Ahmed Sallam, Vamsi C Meesala, Muhammad R Hajj, and Shima Shahab. Holographic mirrors for spatial ultrasound modulation in contactless acoustic energy transfer systems. *Applied Physics Letters*, 119(14), 2021.
- [64] Ahmed Sallam, Ceren Cengiz, Mihir Pewekar, Eric Hoffmann, Wynn Legon, Eli Vlaisavljevich, and Shima Shahab. Gradient descent optimization of acoustic holograms for transcranial focused ultrasound. *Journal of Applied Physics*, 136(14), 2024.
- [65] Vivian Shen, Chris Harrison, and Craig Shultz. Expressive, scalable, mid-air haptics with synthetic jets. *ACM Trans. Comput.-Hum. Interact.*, 31(2), January 2024. ISSN 1073-0516. doi: 10.1145/3635150. URL <https://doi.org/10.1145/3635150>.
- [66] Craig Shultz and Chris Harrison. Lrair: Non-contact haptics using synthetic jets. In *2022 IEEE Haptics Symposium (HAPTICS)*, pages 1–6, 2022. doi: 10.1109/HAPTICS52432.2022.9765565.
- [67] K Kirk Shung and Michael Zippuro. Ultrasonic transducers and arrays. *IEEE Engineering in Medicine and Biology Magazine*, 15(6):20–30, 1996.
- [68] Y. Suzuki and M. Kobayashi. Air jet driven force feedback in virtual reality. *IEEE Computer Graphics and Applications*, 25(1):44–47, 2005. doi: 10.1109/MCG.2005.1.
- [69] Mauricio Tamayo, Pablo J. Salazar, D. Carlos Bustamante, S. Marcelo Silva, V. Miguel Escudero, and Victor H. Andaluz. Virtual rehabilitation of carpal tunnel syndrome through force feedback. In Lucio Tommaso De Paolis and Patrick Bourdot, editors,

- Augmented Reality, Virtual Reality, and Computer Graphics*, pages 153–164, Cham, 2018. Springer International Publishing. ISBN 978-3-319-95282-6.
- [70] Zhenhua Tian, Zeyu Wang, Peiran Zhang, Ty Downing Naquin, John Mai, Yuqi Wu, Shujie Yang, Yuyang Gu, Hunter Bachman, Yaosi Liang, Zhiming Yu, and Tony Jun Huang. Generating multifunctional acoustic tweezers in petri dishes for contactless, precise manipulation of bioparticles. *Science Advances*, 6(37):eabb0494, 2020. doi: 10.1126/sciadv.abb0494. URL <https://www.science.org/doi/abs/10.1126/sciadv.abb0494>.
- [71] Wei Dawid Wang, Zhengbing Ding, Yongkyu Lee, and Xu Han. Engineering liquid-vapor phase transition for refreshable haptic interfaces. *Research*, 2022, 2022. doi: 10.34133/2022/9839815. URL <https://spj.science.org/doi/abs/10.34133/2022/9839815>.
- [72] Malte Weiss, Chat Wacharamanatham, Simon Voelker, and Jan Borchers. Fingerflux: near-surface haptic feedback on tabletops. In *Proceedings of the 24th Annual ACM Symposium on User Interface Software and Technology*, UIST '11, page 615–620, New York, NY, USA, 2011. Association for Computing Machinery. ISBN 9781450307161. doi: 10.1145/2047196.2047277. URL <https://doi.org/10.1145/2047196.2047277>.
- [73] Yanbin Xu, Shengnan Zhang, Xuyang Bao, Dongdong Zheng, and Feng Dong. Amplitude modulation method for acoustic radiation force impulse excitation. *IEEE Transactions on Instrumentation and Measurement*, 69(5):2429–2438, 2020. doi: 10.1109/TIM.2020.2966309.
- [74] Zhen Xu, Timothy L Hall, Eli Vlaisavljevich, and Fred T Lee Jr. Histotripsy: the first noninvasive, non-ionizing, non-thermal ablation technique based on ultrasound. *International Journal of Hyperthermia*, 38(1):561–575, 2021.

- [75] Yu-Feng Zhou. High intensity focused ultrasound in clinical tumor ablation. *World journal of clinical oncology*, 2(1):8, 2011.
- [76] Mounia Ziat. Haptics for human-computer interaction: From the skin to the brain. *Foundations and Trends® in Human-Computer Interaction*, 17(1-2):1–194, 2023. ISSN 1551-3955. doi: 10.1561/11000000061. URL <http://dx.doi.org/10.1561/11000000061>.

Chapter 3

Future Work

An experimental setup has been devised to further confirm the findings obtained from simulation model results by recording the real physical response of a skin-mimicking phantom material subjected to focal scanning. The setup is mostly consistent with similar works [20][56] and has been fully assembled (Fig. 3.1). For the haptic focal point generation, an Ultraleap STRATOS Inspire 256 transducer PAT has been utilized, and is programmed using the Ultrahaptics Core Asset. It is positioned 20cm above the surface of a commercially available viscoelastic gel (Gelatin #2, Humimic), which is a suitable material for vibrometry experiments [56]. The mechanical response on the surface of the gel would then be captured using a Polytec scanning laser Doppler vibrometer.

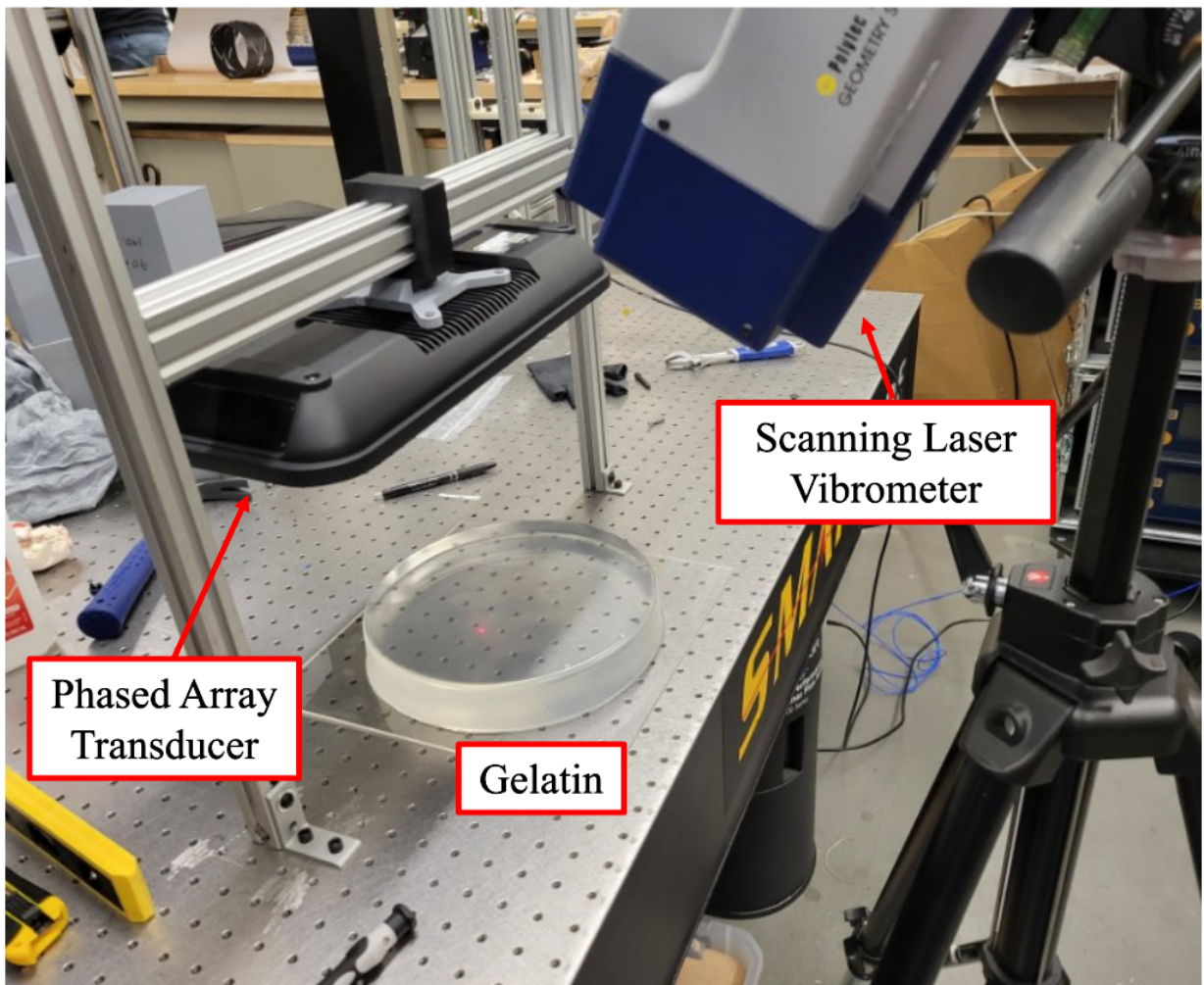


Figure 3.1: Experimental set up, missing reflective powder on the surface of the gel